Quantifying the evolutionary potential and constraints of a drug-targeted viral protein

Lei Dai[1, 2]*, Yushen Du[1]*, Hangfei Qi[1], Nicholas C. Wu[1,3], Ergang Wang[1], James O. Lloyd-Smith[2], Ren Sun[1]

[1]Department of Molecular and Medical Pharmacology

[2]Department of Ecology and Evolutionary Biology, University of California Los Angeles, Los Angeles, United States

[3]Current address: Department of Integrative Structural and Computational Biology, The Scripps Research Institute, La Jolla, United States

*: these authors contributed equally to this study

Corresponding author:

Ren Sun, Ph.D.

Email: rsun@mednet.ucla.edu

Abstract

RNA viruses are notorious for their ability to evolve rapidly under novel environments. It is known that the high mutation rate of RNA viruses can generate huge genetic diversity to facilitate viral adaptation. However, less attention has been paid to the underlying fitness landscape that represents the selection forces on viral genomes. Here we systematically quantified the distribution of fitness effects (DFE) of single amino acid substitutions (86 amino acids total) in the drug-targeted region of NS5A protein of Hepatitis C Virus (HCV). We found that the majority of non-synonymous substitutions incur large fitness costs, suggesting that NS5A protein is highly optimized in natural conditions. Furthermore, we characterized the evolutionary potential of HCV by subjecting the mutant viruses to varying concentrations of an NS5A inhibitor Daclatasvir. As the selection pressure increases, the DFE of beneficial mutations shifts from an exponential distribution to a heavy-tailed distribution with a disproportionate number of exceptionally fit mutants. The number of available beneficial mutations and the selection coefficient are both found to increase at higher levels of antiviral drug concentration, as predicted by a pharmacodynamics model describing viral fitness as a function of drug concentration. Our large-scale fitness data of mutant viruses also provide insights into the biophysical basis of evolutionary constraints and the role of the genetic code in protein evolution.

Introduction

In our evolutionary battles with microbial pathogens, RNA viruses are among the most formidable foes. HIV-1 and Hepatitis C Virus acquire drug resistance in patients under antiviral therapy. Influenza and Ebola virus cross the species barrier to infect human hosts. Understanding the evolution of RNA viruses is therefore of paramount importance for developing antivirals and vaccines and assessing the risk of future emergence events (Domingo et al. 2012; Goldberg et al. 2012; Metcalf et al. 2015). Comprehensive characterization of viral fitness landscapes, and the principles underpinning them, will provide us with a map of evolutionary pathways accessible to RNA viruses and guide our design of effective strategies to limit antiviral resistance, immune escape and cross-species transmission (Turner and Elena 2000; Ke et al. 2015; Barton et al. 2016).

Although the concept of fitness landscapes has been around for a long time (Wright 1932), we still know little about their properties in real biological systems. Previous empirical studies of fitness landscapes have been constrained by very limited sampling of sequence space. In a typical study, mutants are generated by site-directed mutagenesis and assayed for growth rate individually. We and others have recently developed a high-throughput technique, often referred to as “deep mutational scanning”, to profile the fitness effect of mutations by integrating deep sequencing with selection experiments (Wu et al. 2013; Fowler and Fields 2014; Thyagarajan and Bloom 2014). This novel application of next generation sequencing has raised an exciting prospect of large-scale fitness measurements (Qi et al. 2014; Wu et al. 2014; Li et al. 2016; Puchta et al. 2016) and a revolution in our understanding of molecular evolution (He and Liu 2016).

The distribution of fitness effects (DFE) of mutations is a fundamental entity in genetics and reveals the local structure of a fitness landscape (Burch and Chao 2000; Eyre-Walker and Keightley 2007; Hietpas et al. 2011; Desai 2013; Jacquier et al. 2013; Bataillon and Bailey 2014; Bank et al. 2015; Chevereau et al. 2015). Deleterious mutations are usually abundant and impose severe constraints on the accessibility of fitness landscapes. In contrast, beneficial mutations are rare and provide the raw materials of adaptation. Quantifying the DFE of RNA viruses is crucial for understanding how these pathogens evolve to acquire drug resistance and surmount other evolutionary challenges.

The model system used in our study is Hepatitis C Virus (HCV), a positive sense single-stranded RNA virus with a genome of ~9.6 kb. The biology of HCV has been studied extensively in the past two decades and provides an excellent model system of human RNA viruses. We applied high-throughput fitness assays to map the fitness effects of all single amino acid substitutions in domain IA (amino acid 18-103) of HCV NS5A protein (Methods). This domain is the target of several directly-acting antiviral drugs, including

Daclatasvir (DCV) (Gao et al. 2010). We profiled the DFE of HCV NS5A protein under varying levels of positive selection by tuning the concentration of the antiviral drug DCV. In addition, we studied how viral evolution is constrained by deleterious mutations that impact protein stability. Finally, we analyzed the shape of the DFE in nucleotide sequence space and analyzed how the structure of the genetic code influences protein evolution.

Results

Profiling the fitness landscape of HCV NS5A protein

To study the DFE of mutations of HCV NS5A protein, we used a previously constructed library of mutant viruses using saturation mutagenesis (Qi et al. 2014). Briefly, each codon in the mutated region was randomized to cover all possible single amino acid substitutions. We observed 2520 non-synonymous mutations in the plasmid library, which covered 99.6% (1628 out of 1634) of all possible single amino acid substitutions, as well as 105 synonymous mutations. After transfection, we performed selection on the mutant viruses in an HCV cell culture system (Lindenbach et al. 2005). Mutants with frequency below a certain cutoff after transfection were assigned as lethal mutations (Methods). The relative fitness of a mutant virus to the wild-type virus was calculated based on the changes in frequency of the mutant virus and the wild-type virus after one round of selection in cell culture (Supplementary Figure 1).

Our experiment provides a comprehensive profiling of the local fitness landscape of all single amino acid mutations. As expected, the fitness effects of synonymous mutations were nearly neutral, while most non-synonymous mutations were deleterious (Figure 1). After grouping together non-synonymous mutations leading to the same amino acid substitution, we found that around 90% of single amino acid mutations had fitness costs and almost half of them were found to be lethal (Supplementary Figure 2). The high sensitivity to mutations in HCV NS5A, an essential protein for viral replication, is generally consistent with previous mutagenesis studies of RNA viruses (Sanjuan et al. 2004). Our data support the view that RNA viruses are very sensitive to the effect of deleterious mutations, possibly due to the compactness of their genomes (Elena et al. 2006; Rihn et al. 2013).

Using the distribution of fitness effects of synonymous mutations as a benchmark for neutrality, we identified that only 3.4% of single amino acid mutations are beneficial (Methods). The estimated fraction of beneficial mutations is consistent with previous small-scale mutagenesis studies in viruses including bacteriophages, vesicular stomatitis virus, etc. (Sanjuan et al. 2004; Burch et al. 2007; Eyre-Walker and

Keightley 2007; Silander et al. 2007). Our results indicate that HCV NS5A protein is under strong purifying selection, suggesting that viral proteins are highly optimized in their natural conditions.

Evolutionary potential as a function of positive selection

Beneficial mutations are the raw materials of protein adaptation (Eyre-Walker and Keightley 2007). Previous studies have found that the evolvability of proteins is a function of purifying selection (Stiffler et al. 2015). In this study, we aimed to study the role of positive selection in modulating the evolutionary potential of drug-targeted viral proteins. In addition to growing viruses in the natural condition without drugs, we selected the mutant library in 10, 40 and 100 pM of a potent HCV NS5A inhibitor Daclatasvir (DCV). The drug concentrations were chosen based on in vitro IC_{50} of wild type HCV virus (~20 pM) to represent different levels of positive selection (mild, intermediate and strong).

By tuning the concentration of DCV, we observed a shift in the DFE of beneficial mutations (Figure 2A, Supplementary Figure 3). At higher drug concentrations, we observed an increase in the average selection coefficient as well as the total number of beneficial mutations (Table 1). We further tested whether the shape of this distribution changed under drug selection. Previous empirical studies supported the hypothesis that the DFE of beneficial mutations is exponential (Imhof and Schlötterer 2001; Sanjuan et al. 2004; Cowperthwaite et al. 2005; Rokyta et al. 2005; Kassen and Bataillon 2006; Burch et al. 2007; Carrasco et al. 2007; MacLean and Buckling 2009; Peris et al. 2010; Bataillon et al. 2011). Following a maximum likelihood approach, we fit the DFE of beneficial mutations to the Generalized Pareto Distribution (Supplementary Figure 4, Methods). The fitted distribution (Table 1) is described by two parameters: a scale parameter (τ), and a shape parameter (κ) that determines the behavior of the distribution's tail. Using a likelihood-ratio test (Beisel et al. 2007), we found that the distribution was exponential ($\kappa = 0$) in the natural condition without drug selection, but shifted to a heavy-tailed distribution ($\kappa > 0$) in the presence of DCV, a condition that the wild type virus was poorly adapted to. Our observation confirms the prediction that the shape of the DFE of beneficial mutations is dependent on how well adapted the wild type is in a certain environment (Eyre-Walker and Keightley 2007). When individuals encounter novel environments (i.e. novel forms of selection pressure) (Rokyta et al. 2008; Schenk et al. 2012), the fitness of the wild type is no longer top-ranking and the DFE is expected to deviate from the exponential distribution (MacLean et al. 2010).

A simple pharmacodynamics model describing viral fitness as a function of drug concentration (i.e. phenotype-fitness mapping) can explain the changing spectra of beneficial mutations upon drug treatment (Figure 2B). For example, mutations that reduce a protein's binding affinity to drug molecules (i.e. with a higher inhibitory concentration than wild-type) may come with a fitness cost (Wu et al. 2013). Thus, a drug-resistant mutant that is deleterious in the absence of drug may become beneficial under drug selection, leading to an increase in the number of beneficial mutations. Moreover, the relative fitness of the drug-resistant mutant is expected to increase with stronger selection pressure (Figure 2B, dashed line).

The dose response curves were previously measured for a set of mutants constructed by site-directed mutagenesis (Supplementary Figure 5) (Qi et al. 2014). Indeed, we found that the relative fitness of drug-resistant mutants increased at higher drug concentration (Figure 2C); in contrast, drug-sensitive mutants became less fit under drug selection. Furthermore, based on this set of mutants with validated dose response curves, we were able to use the fitness measurements to estimate the IC_{50} of all mutants in our library (Supplementary Figure 6, Methods). In particular, we found that a small group of mutations were highly resistant to DCV and this could explain the heavy-tailed DFE of beneficial mutations under drug selection. Overall, our results suggest that the evolutionary potential of proteins is modulated by the strength of positive selection, in addition to the previous findings on the role of purifying selection (Stiffler et al. 2015).

Deleterious mutations as evolutionary constraints

While beneficial mutations open up adaptive pathways to genotypes with higher fitness, mutations that reduce fitness impose constraints on the evolution of viruses. To understand the biophysical basis of mutational effects (Liberles et al. 2012), we took advantage of the available structural information. The crystal structure of NS5A domain I is available excluding the amphipathic helix at N-terminus (Tellinghuisen et al. 2005; Love et al. 2009).

We found that the fitness effects of deleterious mutations at buried sites (i.e. with lower solvent accessibility) were more pronounced than those at surface exposed sites (Figure 3A, Supplementary Figure 7) (Ramsey et al. 2011). Moreover, we performed simulations of protein stability for individual mutants using the PyRosetta program (Methods) (Das and Baker 2008; Chaudhury et al. 2010). A mutation with $\Delta\Delta G>0$, i.e. shifting the free energy difference to favor the unfolded state, is expected to destabilize the protein. We found that mutations that decreased protein stability led to reduced viral fitness (Figure 3B). For example, mutations at a stretch of highly conserved residues (F88-N91) that run through the core of NS5A protein tended to destabilize the protein and significantly reduced the viral fitness (Supplementary Figure 8). Mutations that increase $\Delta\Delta G$ beyond a threshold were mostly lethal. This is consistent with the threshold robustness model, which predicts that proteins become unfolded after using up the stability margin (Bloom et al. 2005; Wylie and Shakhnovich 2011; Olson et al. 2014). In contrast, mutations at some sites were highly deleterious despite having little impact on protein stability, suggesting that evolution at these sites may be under additional constraints to preserve protein function (Wu et al. 2015; Echave et al. 2016; Jack et al. 2016), such as RNA binding (Foster et al. 2010; Hwang et al. 2010).

We further tested whether the viral replication fitness in cell culture was predictive of evolutionary landscapes of viruses in patients (Ferguson et al. 2013). This is critical for the extrapolation of viral replication fitness from in vitro to in vivo (Hart and Ferguson 2015). We analyzed sequence diversity of HCV sequences in the database of Los Alamos National Lab (Methods). Indeed, we found that the within-patient sequence diversity at each site was highly correlated to the replication fitness measured in cell culture (Spearman's ρ=0.82, Figure 3C), suggesting that fitness landscapes profiled in laboratory settings can provide insights into evolutionary pathways of viruses in nature (Gong et al. 2013).

The role of the genetic code in protein evolution

So far we have considered the spectrum of beneficial and deleterious mutations in the amino acid sequence space (Wu et al. 2016). In fact, the evolution of viral proteins in the nucleotide sequence space faces additional constraints posed by the genetic code, because most mutations in RNA viruses occur as point mutations during genome replication. Our fitness data of single codon mutants (replaced by NNK) provides a unique opportunity to examine impacts of the genetic code on the evolution of proteins (Firnberg and Ostermeier 2013).

Due to codon degeneracy, many point mutations are synonymous and thus less likely to be deleterious than 2 or 3-nt substitutions. For non-synonymous mutations, we found that the deleterious impacts on fitness increased with the number of nucleotide substitutions (Figure 4A, B), supporting the hypothesis that the structure of the standard genetic code can buffer the mutational load (Firnberg and Ostermeier 2013). This observation is consistent with the facts that amino acids with similar biochemical properties tend to be adjacent in the genetic code (Yampolsky and Stoltzfus 2005), and that mutating to biochemically similar amino acids is less likely to decrease fitness (Supplementary Figure 2).

For HCV and other RNA viruses, there is an observed transition:transversion bias in evolution (Tanaka et al. 1993; Duchêne et al. 2015). This phenomenon has been attributed to two different, but not mutually exclusive, causes: 1) the "mutation hypothesis" argues for a transition:transversion bias in the mutation rate, which is bolstered by experimental measurement of de novo mutation rates in viruses (Acevedo et al. 2014); 2) the "selection hypothesis" argues that natural selection favors amino acid replacements via transition (Stoltzfus and Norris 2016). We tested the "selection hypothesis" using the non-synonymous point mutations in our library (Figure 4D). We found that the fraction of lethal mutations caused by transversions was slightly larger than transitions, but the difference was not statistically significant. Together with previous studies in other systems (Stoltzfus and Norris 2016), our results suggest that the "selection hypothesis" is unlikely to be the major cause underlying the transition:transversion bias in evolution of viral proteins.

In addition, we observed a slight (though not statistically significant) enrichment of beneficial mutations in point mutations under the natural condition (Figure 4C). Under drug selection, our conclusions on the shifting DFE of beneficial single amino acid mutations still held true for point mutations (Supplementary Figure 9, Supplementary Table 1). Furthermore, we observed that beneficial mutations were significantly depleted in 3-nt substitutions (Supplementary Figure 10). However, this difference in the fraction of beneficial mutations can be confounded by the fact that 3-nt substitutions are more likely to be lethal. As pointed out in a previous study on the potential benefits of the genetic code in protein evolution (Firnberg and Ostermeier 2013), mutational robustness and the enrichment of beneficial mutations may actually be two sides of the same coin.

Discussion

Mutation accumulation (Levy et al. 2015) and site-directed mutagenesis (Visher et al. 2016) are traditional approaches to examine the DFE. Both methods provide pivotal insights into the shape of the DFE, yet with limitations. The site-directed mutagenesis approach requires fitness assays for each mutant and can only provide a sparse sampling of mutations. The sampling of sequence space in a mutation accumulation experiment is biased towards large-effect beneficial mutations, as they are more likely to fix in the population. In contrast, the "deep mutational scanning" approach (Wu et al. 2013; Fowler and Fields 2014), which utilizes high-throughput sequencing to simultaneously assay the fitness or phenotype of a library of mutants, allows for unbiased and large-scale sampling of fitness landscapes and thus is ideal for studying the characteristics of empirical DFE.

The shape of the DFE determines mutational robustness (Visser et al. 2003; Draghi et al. 2010; Visher et al. 2016). Our study quantified the fitness effects of single amino acid substitutions in the drug-targeted region of an essential viral protein (86 amino acids, 1628 out of 1634 possible substitutions). In general, the empirical DFE of HCV NS5A was consistent with previous findings that viral proteins were highly optimized in the natural condition and very sensitive to the effects of deleterious mutations. Moreover, given the advantages of our saturation mutagenesis, we were able to use the fitness data to test multiple hypotheses of protein evolution, including the role of the genetic code in buffering mutational load, and the cause of transition:transversion bias. In the future, profiling the DFE in a range of different systems will allow us to test the generality of our conclusions.

In our study, we have used the fitness effects of synonymous mutations to determine the threshold of neutrality. Synonymous mutations are usually expected to have no or minimal influence on phenotype or fitness, but this view is being increasingly challenged as the effect of synonymous mutations on protein expression and folding becomes elucidated, such as via mRNA secondary structures or codon usage (Yang et al. 2014; Agashe et al. 2016). One interesting observation in our selection experiments is that some synonymous mutations seemed to have phenotypic effects on drug sensitivity (Supplementary Figure 11). Although this is not the focus of our study, understanding the mechanism of natural selection at the RNA level and its implications for molecular evolution, particularly in the context of RNA viruses, may be a fruitful area for future studies.

One often overlooked point is that DFE will vary as a function of selection pressure (Martin and Lenormand 2006; Lalić et al. 2011; Stiffler et al. 2015). For example, mutations that impair function would become more deleterious with increasing pressure of purifying selection, thus leading to reduced protein evolvability (Stiffler et al. 2015). In this study, we have focused on gain-of-function mutations in a novel environment. The pleiotropic effect of mutations causes the spectrum of beneficial mutations to shift between the natural condition and the condition with drug selection. Moreover, mutations enabling the new function (e.g. drug resistance) become more beneficial with increasing pressure of positive selection.

Although different systems have distinct protein-drug interactions that lead to different resistance profiles (Robinson et al. 2011), the results in our study provide a general framework to study DFE of drug-targeted proteins. Future studies along this line will further our understanding of how proteins evolve new functions under the constraint of maintaining their original function (Soskine and Tawfik 2010), as exemplified in the evolution of resistance to directly-acting antiviral drugs (Rosenbloom et al. 2012). We have also demonstrated that the fitness data could be utilized to infer drug sensitivity of mutants and inform predictive modeling of within-patient viral dynamics (Ke et al. 2015). Quantifying the characteristics of DFE of drug-targeted proteins under different environments (e.g. varying levels of selection pressure, or conflicting selection pressures), would allow us to assess repeatability in the outcomes of viral evolution (de Visser and Krug 2014) and guide the design of therapies to minimize drug resistance (Ogbunugafor et al. 2016).

Conclusions

Many RNA viruses adapt rapidly to novel selection pressures, such as antiviral drugs. Understanding how pathogens evolve under drug selection is critical for the success of antiviral therapy against human pathogens. By combining deep sequencing with selection experiments in cell culture, we have quantified the distribution of fitness effects of mutations in the drug-targeted domain of Hepatitis C Virus NS5A protein. Our results indicate that the majority of single amino acid substitutions in NS5A protein incur large fitness costs. Combined with stability predictions based on protein structure, our fitness data reveal the biophysical constraints underlying the evolution of viral proteins. Furthermore, by subjecting the mutant viruses to positive selection under an antiviral drug, we find that the evolutionary potential of viral proteins in a novel environment is modulated by the strength of selection pressure.

Materials and Methods

Mutagenesis

The mutant library of HCV NS5A protein domain IA (86 amino acids) was constructed using saturation mutagenesis as previously described (Qi et al. 2014). In brief, the entire region was divided into five sub-libraries each containing 17-18 amino acids. NNK (N: A/T/C/G, K: T/G) was used to replace each amino acid. The oligos, each of which contains one random codon, were synthesized by IDT. The mutated region was ligated to the flanking constant regions, subcloned into the pFNX-HCV plasmid and then transformed into bacteria. The pFNX-HCV plasmid carrying the viral genome was synthesized in Dr. Ren Sun's lab based on the chimeric sequence of genotype 2a HCV strains J6/JFH1.

Cell culture

The human hepatoma cell line (Huh-7.5.1) was provided by Dr. Francis Chisari from the Scripps Research Institute, La Jolla. The cells were cultured in T-75 tissue culture flasks (Genesee Scientific) at 37 ^{o}C with 5% CO_2. The complete growth medium contained Dulbecco's Modified Eagle's Medium (Corning Cellgro), 10% heat inactivated Fetal Bovine Serum (Omega Scientific), 10 mM HEPES (Life Technologies), 1x MEM Non-Essential Amino Acids Solution (Life Technologies) and 1x Penicillin-Streptomycin-Glutamine (Life Technologies).

Selection

Plasmid mutant library was transcribed in vitro using T7 RiboMAX Express Large Scale RNA Production System (Promega) and purified by PureLink RNA Mini Kit (Life Technologies). 10 μg of in vitro transcribed RNA was used to transfect 4 million Huh-7.5.1 cells via electroporation by Bio-Rad Gene Pulser (246 V, 950 μF). The supernatant was collected 144 hours post transfection and virus titer was determined by immunofluorescence assay. The viruses collected after transfection were used to infect ~2 million Huh-7.5.1 cells with an MOI at around 0.1-0.2. The five mutant libraries were passaged for selection separately as previously described (Qi et al. 2015). For the three different levels of selection pressure, the growth media was supplemented with 10 pM, 40 pM and 100 pM HCV NS5A inhibitor Daclatasvir (BMS-790052), respectively. The supernatant was collected at 144 hours post infection.

Preparation of Illumina sequencing samples

For each sample, viral RNA was extracted from 700 µl supernatant collected after transfection and after selection using QIAamp Viral RNA Mini Kit (Qiagen). Extracted RNA was reverse transcribed into cDNA by SuperScript III Reverse Transcriptase Kit (Life Technologies). The targeted region in NS5A (51-54 nt) was PCR amplified using KOD Hot Start DNA polymerase (Novagen). The Eppendorf thermocycler was set as following: 2 min at 95 °C; 25 to 35 three-step cycles of 20 s at 95 °C,15 s at 52-56 °C (sub-library #1, 52 °C; #2, 52 °C; #3, 52 °C; #4, 56 °C; #5, 54 °C) and 25s at 68 °C; 1 min at 68 °C. The number of PCR cycles are chosen based on the copy number of cDNA templates as determined by qPCR (Bio-Rad). The PCR primers are listed in Table S1. The PCR products were purified using PureLink PCR Purification Kit (Life Technologies) and prepared for Illumina Hiseq 2000 sequencing (paired-end 100 bp) following 5'-phosphorylation using T4 Polynucleotide Kinase (New England BioLabs), 3' dA-tailing using dA-tailing module (New England BioLabs), and TA ligation of the adapter using T4 DNA ligase (Life Technologies). Each sample was tagged with a unique 3-bp customized barcodes, which were part of the adapter sequence and were sequenced as the first three nucleotides in both the forward and reverse reads (Wu et al. 2015) (Table S2).

Analysis of sequencing data

The sequencing data were parsed by SeqIO function of BioPython. The reads from different samples were de-multiplexed by the barcodes and mapped to the entire mutated region in NS5A by allowing at maximum 5 mismatches with the reference genome (Table S3) (Qi et al. 2014). Since both forward and reverse reads cover the whole amplicon, we used paired reads to correct for sequencing errors. A mutation was called only if it was observed in both reads and the quality score at the corresponding position was at least 30. Sequencing reads containing mutations not supposed to appear in the mutant library were excluded from downstream analysis. The sequencing depth for each sub-library is at least ~10^5 and two orders of magnitude higher than the library complexity.

Calculation of relative fitness

For each condition of selection experiments (i.e. different concentration of Daclatasvir [DCV]), the relative fitness (RF) of a mutant virus to the wild-type virus is calculated by the relative changes in frequency after selection,

$$RF_{mut}([DCV]) = \left(\frac{f_{mut}^{T=1}}{f_{mut}^{T=0}}\right) \Bigg/ \left(\frac{f_{WT}^{T=1}}{f_{WT}^{T=0}}\right)$$

where $f_{mut}^{T=round}$ and $f_{WT}^{T=round}$ is the frequency of the mutant virus and the wild-type virus at round 0 (after transfection) or round 1 (after selection). The fitness of wild-type virus is normalized to 1. The fitness values estimated from one round have been shown to be highly consistent to estimates from multiple rounds of selection (Qi et al. 2014).

Mutants with less than 10 read counts in the plasmid library were filtered. A mutation was considered lethal if at least one of the two criteria was met: 1) after transfection, the mutant had less than 10 read counts; 2) after transfection, the ratio between the mutant's frequency and the wild-type's frequency was smaller than 10^{-4}. The thresholds for beneficial and deleterious mutations were defined as $1+2\sigma_{silent}$ and $1-2\sigma_{silent}$, respectively. σ_{silent} is the standard deviation of the fitness effects of synonymous mutations under the natural condition (Figure 1). The fitness effects of non-synonymous mutations leading to the same amino acid substitution were averaged to estimate the fitness effect of the given single amino acid substitution.

Fitting the distribution of fitness effects of beneficial mutations

The distribution of selection coefficients of beneficial mutations were fitted to a Generalized Pareto Distribution following a maximum likelihood approach (Beisel et al. 2007),

$$F(x|\kappa,\tau)=$$

$$\begin{cases} 1-(1+\frac{\kappa}{\tau}x)^{-1/\kappa}, x\geq 0, \ \ if\,\kappa>0 & \text{(Frechet)} \\ 1-(1+\frac{\kappa}{\tau}x)^{-1/\kappa}, 0\leq x<-\frac{\tau}{\kappa}, \ \ if\,\kappa<0 & \text{(Weibull)} \\ 1-e^{-x/\tau}, x\geq 0, \ \text{if}\ \kappa=0 & \text{(Gumbel)} \end{cases}$$

Only mutations with relative fitness higher than the beneficial threshold $1+2\sigma_{silent}$ were included in the distribution of beneficial mutations. The selection coefficients were normalized to the beneficial threshold. The shape parameter κ determines the tail behavior of the distribution, which can be divided into three domains of attraction: Gumbel domain (exponential tail, κ = 0), Weibull domain (truncated tail, κ < 0) and Fréchet domain (heavy tail, κ > 0). For each selection condition, a likelihood ratio test is performed to evaluate whether the null hypothesis κ = 0 (exponential distribution) can be rejected.

Estimation of IC_{50} from fitness data

We can quantify the drug resistance of each mutant in the library by computing its fold change in relative fitness,

$$W([DCV])=\frac{RF_{mut}([DCV])}{RF_{mut}}$$

Here RF_{mut} is the relative fitness of a mutant under the natural condition (i.e. no drug). W is the fold change in relative fitness and represents the level of drug resistance relative to the wild type. W > 1 indicates drug resistance, and W < 1 indicates drug sensitivity.

This empirical measure of drug resistance can be directly linked to a simple pharmacodynamics model (Rosenbloom et al. 2012), where the viral replicative fitness is modeled as a function of drug dose,

$$W([DCV]) = \frac{RF_{mut}([DCV])}{RF_{mut}} = \left(\frac{IC_{mut}}{[DCV]+IC_{mut}}\right) \Big/ \left(\frac{IC_{wt}}{[DCV]+IC_{wt}}\right)$$

Here IC denotes the half-inhibitory concentration. The Hill coefficient describing the sigmoidal shape of the dose response curve is fixed to 1, as used in fitting the dose response curves of wild-type virus and validated mutant viruses (Supplementary Figure 5). We can use the drug resistance score W to infer the dose response of each mutant. Because the dose response curve depends on the duration of drug treatment, we transformed $W_{observed}$ (144 hr drug treatment in selection experiments) to $W_{predicted}$ (48 hr drug treatment, Supplementary Figure 6A) and then calculated IC_{50} using the equation above.

Calculation of relative solvent accessibility

DSSP (http://www.cmbi.ru.nl/dssp.html) was used to compute the Solvent Accessible Surface Area (SASA) (Kabsch and Sander 1983) from the HCV NS5A protein structure (PDB: 3FQM) (Love et al. 2009). SASA was then normalized to Relative Solvent Accessibility (RSA) using the empirical scale reported in (Tien et al. 2013).

Predictions of protein stability

ΔΔG (in Rosetta Energy Units) of HCV NS5A mutants was predicted by PyRosetta (version: “monolith.ubuntu.release-104”) as the difference in scores between the monomer structure of mutants (single amino acid mutations from site 32 to 103) and the reference (PDB: 3FQM). The score is designed to capture the change in thermodynamic stability caused by the mutation (ΔΔG) (Das and Baker 2008). The sequence of the reference protein was different from the sequence of the wild-type virus used in this study. Thus instead of directly comparing ΔΔG to fitness effects, we used the median ΔΔG caused by amino acid substitutions at each site.

The PDB file of NS5A dimer was cleaned and trimmed to a monomer (chain A). Next, all side chains were repacked (sampling from the 2010 Dunbrack rotamer library (Shapovalov and Dunbrack 2011)) and minimized for the reference structure using the talaris2014 scoring function. After an amino acid mutation was introduced, the mutated residue was repacked, followed by quasi-Newton minimization of the backbone and all side chains (algorithm: “lbfgs_armijo_nonmonotone”). This procedure was performed 50 times, and the predicted ΔG of a mutant structure is the average of the three lowest scoring structures.

We note that predictions based on NS5A monomer structure were only meant to provide a crude profile of how mutations at each site may impact protein stability. Potential structural constraints at the dimer interface have been ignored, which is further complicated by the observations of two different NS5A dimer structures (Tellinghuisen et al. 2005; Love et al. 2009). The reference sequence of NS5A in the PDB file (PDB: 3FQM) is different from the WT sequence used in our experiment by 20 amino acid substitutions.

Within-patient sequence diversity

Aligned nucleotide sequences of HCV NS5A protein were downloaded from Los Alamos National Lab database (Kuiken et al. 2005) (all HCV genotypes, ~2600 sequences total) and clipped to the region of interest (amino acid 18-103 of NS5A). Sequences that caused gaps in the alignment of H77 reference genome were manually removed. After translation to amino acid sequences, sequences with ambiguous amino acids were removed (~2300 amino acid sequences after filtering). The sequence diversity at each amino acid site was quantified by Shannon entropy.

Acknowledgements

L.D. was supported by HHMI Postdoctoral Fellowship from Jane Coffin Childs Memorial Fund for Medical Research. N.C.W. was supported by Croucher Foundation Fellowship. R.S. was supported by NSFC 81172314, NIH DE023591 and NIH CA177322.

Author contributions

L.D., Y.S., H.Q. and R.S. designed the experiments. L.D., H.Q. and Y.S. performed the experiments. L.D. and Y.S. analyzed the experimental data. L.D. performed the bioinformatics analyses on sequence diversity and protein structure. L.D., E.W. and Y.S. performed the molecular modeling. L.D. wrote the first draft of the manuscript. All authors discussed the results and commented on the manuscript.

References

Acevedo A, Brodsky L, Andino R. 2014. Mutational and fitness landscapes of an RNA virus revealed through population sequencing. Nature 505:686–690.

Agashe D, Sane M, Phalnikar K, Diwan GD, Habibullah A, Martinez-Gomez NC, Sahasrabuddhe V, Polachek W, Wang J, Chubiz LM, et al. 2016. Large-Effect Beneficial Synonymous Mutations Mediate Rapid and Parallel Adaptation in a Bacterium. Mol. Biol. Evol. 33:1542–1553.

Bank C, Hietpas RT, Jensen JD, Bolon DNA. 2015. A systematic survey of an intragenic epistatic landscape. Mol. Biol. Evol. 32:229–238.

Barton JP, Goonetilleke N, Butler TC, Walker BD, McMichael AJ, Chakraborty AK. 2016. Relative rate and location of intra-host HIV evolution to evade cellular immunity are predictable. Nat. Commun. 7:11660.

Bataillon T, Bailey S. 2014. Effects of new mutations on fitness: insights from models and data. Ann. New York Acad. … 1320:76–92.

Bataillon T, Zhang T, Kassen R. 2011. Cost of adaptation and fitness effects of beneficial mutations in Pseudomonas fluorescens. Genetics 189:939–949.

Beisel CJ, Rokyta DR, Wichman HA, Joyce P. 2007. Testing the extreme value domain of attraction for distributions of beneficial fitness effects. Genetics 176:2441–2449.

Bloom JD, Silberg JJ, Wilke CO, Drummond DA, Adami C, Arnold FH. 2005. Thermodynamic prediction of protein neutrality. Proc. Natl. Acad. Sci. U. S. A. 102:606–611.

Burch C, Guyader S, Samarov D, Shen H. 2007. Experimental estimate of the abundance and effects of nearly neutral mutations in the RNA virus ϕ6. Genetics 476:467–476.

Burch CL, Chao L. 2000. Evolvability of an RNA virus is determined by its mutational neighbourhood. Nature 406:625–628.

Carrasco P, Iglesia F de la, Elena S. 2007. Distribution of fitness and virulence effects caused by single-nucleotide substitutions in Tobacco etch virus. J. Virol. 81:12979–12984.

Chaudhury S, Lyskov S, Gray JJ. 2010. PyRosetta: a script-based interface for implementing molecular modeling algorithms using Rosetta. Bioinformatics 26:689–691.

Chevereau G, Dravecká M, Batur T, Guvenek A, Ayhan DH, Toprak E, Bollenbach T. 2015. Quantifying the Determinants of Evolutionary Dynamics Leading to Drug Resistance. PLoS Biol. 13:e1002299.

Cowperthwaite MC, Bull JJ, Meyers LA. 2005. Distributions of beneficial fitness effects in RNA. Genetics 170:1449–1457.

Das R, Baker D. 2008. Macromolecular Modeling with Rosetta. Annu. Rev. Biochem. 77:363–382.

Desai MM. 2013. Statistical questions in experimental evolution. J. Stat. Mech. Theory Exp. 2013:P01003.

Domingo E, Sheldon J, Perales C. 2012. Viral quasispecies evolution. Microbiol. Mol. Biol. Rev. 76:159–216.

Draghi JA, Parsons TL, Wagner GP, Plotkin JB. 2010. Mutational robustness can facilitate adaptation. Nature 463:353–355.

Duchêne S, Ho SY, Holmes EC. 2015. Declining transition/transversion ratios through time reveal limitations to the accuracy of nucleotide substitution models. BMC Evol. Biol. 15:312.

Echave J, Spielman SJ, Wilke CO. 2016. Causes of evolutionary rate variation among protein sites. Nat. Rev. Genet. 17:109–121.

Elena SF, Carrasco P, Daròs J-A, Sanjuán R. 2006. Mechanisms of genetic robustness in RNA viruses. EMBO Rep. 7:168–173.

Eyre-Walker A, Keightley PD. 2007. The distribution of fitness effects of new mutations. Nat. Rev. Genet. 8:610–618.

Ferguson AL, Mann JK, Omarjee S, Ndung'u T, Walker BD, Chakraborty AK. 2013. Translating HIV sequences into quantitative fitness landscapes predicts viral vulnerabilities for rational immunogen design. Immunity 38:606–617.

Firnberg E, Ostermeier M. 2013. The genetic code constrains yet facilitates Darwinian evolution. Nucleic Acids Res. 41:7420–7428.

Foster TL, Belyaeva T, Stonehouse NJ, Pearson AR, Harris M. 2010. All three domains of the hepatitis C virus nonstructural NS5A protein contribute to RNA binding. J. Virol. 84:9267–9277.

Fowler DM, Fields S. 2014. Deep mutational scanning: a new style of protein science. Nat. Methods 11:801–807.

Gao M, Nettles RE, Belema M, Snyder LB, Nguyen VN, Fridell R a, Serrano-Wu MH, Langley DR, Sun J-H, O'Boyle DR, et al. 2010. Chemical genetics strategy identifies an HCV NS5A inhibitor with a potent clinical effect. Nature 465:96–100.

Goldberg DE, Siliciano RF, Jacobs WR. 2012. Outwitting evolution: fighting drug-resistant TB, malaria, and HIV. Cell 148:1271–1283.

Gong LI, Suchard MA, Bloom JD. 2013. Stability-mediated epistasis constrains the evolution of an influenza protein. Elife 2:e00631.

Hart GR, Ferguson AL. 2015. Error catastrophe and phase transition in the empirical fitness landscape of HIV. Phys. Rev. E 91:32705.

He X, Liu L. 2016. Toward a prospective molecular evolution. Science 352:769–770.

Hietpas RT, Jensen JD, Bolon DNA. 2011. Experimental illumination of a fitness landscape. Proc. Natl. Acad. Sci. U. S. A. 108:7896–7901.

Hwang J, Huang L, Cordek DG, Vaughan R, Reynolds SL, Kihara G, Raney KD, Kao CC, Cameron CE. 2010. Hepatitis C virus nonstructural protein 5A: biochemical characterization of a novel structural class of RNA-binding proteins. J. Virol. 84:12480–12491.

Imhof M, Schlötterer C. 2001. Fitness effects of advantageous mutations in evolving Escherichia coli populations. Proc. Natl. Acad. Sci. U. S. A. 98:1113–1117.

Jack BR, Meyer AG, Echave J, Wilke CO. 2016. Functional Sites Induce Long-Range Evolutionary Constraints in Enzymes. PLoS Biol. 14:e1002452.

Jacquier H, Birgy A, Le Nagard H, Mechulam Y, Schmitt E, Glodt J, Bercot B, Petit E, Poulain J, Barnaud G, et al. 2013. Capturing the mutational landscape of the beta-lactamase TEM-1. Proc. Natl. Acad. Sci. U. S. A. 110:13067–13072.

Kabsch W, Sander C. 1983. Dictionary of protein secondary structure: Pattern recognition of hydrogen-bonded and geometrical features. Biopolymers 22:2577–2637.

Kassen R, Bataillon T. 2006. Distribution of fitness effects among beneficial mutations before selection in experimental populations of bacteria. Nat. Genet. 38:484–488.

Ke R, Loverdo C, Qi H, Sun R, Lloyd-Smith JO. 2015. Rational Design and Adaptive Management of Combination Therapies for Hepatitis C Virus Infection. PLoS Comput. Biol. 11:e1004040.

Kuiken C, Yusim K, Boykin L, Richardson R. 2005. The Los Alamos hepatitis C sequence database. Bioinformatics 21:379–384.

Lalić J, Cuevas JM, Elena SF. 2011. Effect of host species on the distribution of mutational fitness effects for an RNA virus. PLoS Genet. 7:e1002378.

Levy SF, Blundell JR, Venkataram S, Petrov DA, Fisher DS, Sherlock G. 2015. Quantitative evolutionary dynamics using high-resolution lineage tracking. Nature advance on.

Li C, Qian W, Maclean CJ, Zhang J. 2016. The fitness landscape of a tRNA gene. Science 352:837–840.

Liberles DA, Teichmann SA, Bahar I, Bastolla U, Bloom J, Bornberg-Bauer E, Colwell LJ, de Koning APJ, Dokholyan N V., Echave J, et al. 2012. The interface of protein structure, protein biophysics, and molecular evolution. Protein Sci. 21:769–785.

Lindenbach BD, Evans MJ, Syder AJ, Wölk B, Tellinghuisen TL, Liu CC, Maruyama T, Hynes RO, Burton DR, McKeating JA, et al. 2005. Complete replication of hepatitis C virus in cell culture. Science 309:623–626.

Love RA, Brodsky O, Hickey MJ, Wells PA, Cronin CN. 2009. Crystal structure of a novel dimeric form of NS5A domain I protein from hepatitis C virus. J. Virol. 83:4395–4403.

MacLean RC, Buckling A. 2009. The distribution of fitness effects of beneficial mutations in Pseudomonas aeruginosa. PLoS Genet. 5:e1000406.

MacLean RC, Hall AR, Perron GG, Buckling A. 2010. The population genetics of antibiotic resistance: integrating molecular mechanisms and treatment contexts. Nat. Rev. Genet. 11:405–414.

Martin G, Lenormand T. 2006. The fitness effect of mutations across environments: a survey in light of fitness landscape models. Evolution 60:2413–2427.

Metcalf CJE, Birger RB, Funk S, Kouyos RD, Lloyd-Smith JO, Jansen VAA. 2015. Five challenges in evolution and infectious diseases. Epidemics 10:40–44.

Ogbunugafor CB, Wylie CS, Diakite I, Weinreich DM, Hartl DL. 2016. Adaptive Landscape by Environment Interactions Dictate Evolutionary Dynamics in Models of Drug Resistance. PLoS Comput. Biol. 12:e1004710.

Olson CA, Wu NC, Sun R. 2014. A comprehensive biophysical description of pairwise epistasis throughout an entire protein domain. Curr. Biol. 24:2643–2651.

Peris JB, Davis P, Cuevas JM, Nebot MR, Sanjuán R. 2010. Distribution of fitness effects caused by single-nucleotide substitutions in bacteriophage f1. Genetics 185:603–609.

Puchta O, Cseke B, Czaja H, Tollervey D, Sanguinetti G, Kudla G. 2016. Network of epistatic interactions within a yeast snoRNA. Science 352:840–844.

Qi H, Olson CA, Wu NC, Du Y, Sun R. 2015. Determining the Relative Fitness Score of Mutant Viruses in a Population Using Illumina Paired-end Sequencing and Regression Analysis. Bio-protocol 5:e1475.

Qi H, Olson CA, Wu NC, Ke R, Loverdo C, Chu V, Truong S, Remenyi R, Chen Z, Du Y, et al. 2014. A quantitative high-resolution genetic profile rapidly identifies sequence determinants of hepatitis C viral fitness and drug sensitivity. PLoS Pathog. 10:e1004064.

Ramsey DC, Scherrer MP, Zhou T, Wilke CO. 2011. The Relationship Between Relative Solvent Accessibility and Evolutionary Rate in Protein Evolution. Genetics 188:479–488.

Rihn SJ, Wilson SJ, Loman NJ, Alim M, Bakker SE, Bhella D, Gifford RJ, Rixon FJ, Bieniasz PD. 2013. Extreme genetic fragility of the HIV-1 capsid. PLoS Pathog. 9:e1003461.

Robinson M, Tian Y, Delaney WE, Greenstein AE. 2011. Preexisting drug-resistance mutations reveal unique barriers to resistance for distinct antivirals. Proc. Natl. Acad. Sci. U. S. A. 108:10290–10295.

Rokyta D, Beisel C, Joyce P. 2008. Beneficial fitness effects are not exponential for two viruses. J. Mol. Evol.

67:368–376.

Rokyta D, Joyce P, Caudle S, Wichman H. 2005. An empirical test of the mutational landscape model of adaptation using a single-stranded DNA virus. Nat. Genet. 37:441–444.

Rosenbloom DIS, Hill AL, Rabi SA, Siliciano RF, Nowak MA. 2012. Antiretroviral dynamics determines HIV evolution and predicts therapy outcome. Nat. Med. 18:1378–1385.

Sanjuan R, Moya A, Elena SF. 2004. The distribution of fitness effects caused by single-nucleotide substitutions in an RNA virus. Proc. Natl. Acad. Sci. 101:8396–8401.

Schenk MF, Szendro IG, Krug J, de Visser JAGM. 2012. Quantifying the adaptive potential of an antibiotic resistance enzyme. PLoS Genet. 8:e1002783.

Shapovalov M V, Dunbrack RL. 2011. A smoothed backbone-dependent rotamer library for proteins derived from adaptive kernel density estimates and regressions. Structure 19:844–858.

Silander O, Tenaillon O, Chao L. 2007. Understanding the evolutionary fate of finite populations: the dynamics of mutational effects. PLoS Biol 5.

Soskine M, Tawfik DS. 2010. Mutational effects and the evolution of new protein functions. Nat. Rev. Genet. 11:572–582.

Stiffler MA, Hekstra DR, Ranganathan R. 2015. Evolvability as a Function of Purifying Selection in TEM-1 β-Lactamase. Cell 160:882–892.

Stoltzfus A, Norris RW. 2016. On the Causes of Evolutionary Transition:Transversion Bias. Mol. Biol. Evol. 33:595–602.

Tanaka T, Kato N, Hijikata M, Shimotohno K. 1993. Base transitions and base transversions seen in mutations among various types of the hepatitis C viral genome. FEBS Lett. 315:201–203.

Tellinghuisen TL, Marcotrigiano J, Rice CM. 2005. Structure of the zinc-binding domain of an essential component of the hepatitis C virus replicase. Nature 435:374–379.

Thyagarajan B, Bloom JD. 2014. The inherent mutational tolerance and antigenic evolvability of influenza hemagglutinin. Elife 3.

Tien MZ, Meyer AG, Sydykova DK, Spielman SJ, Wilke CO. 2013. Maximum allowed solvent accessibilites of residues in proteins. PLoS One 8:e80635.

Turner PE, Elena SF. 2000. Cost of Host Radiation in an RNA Virus. Genetics 156:1465–1470.

Visher E, Whitefield SE, McCrone JT, Fitzsimmons W, Lauring AS. 2016. The Mutational Robustness of Influenza A Virus. PLOS Pathog. 12:e1005856.

de Visser JAGM, Krug J. 2014. Empirical fitness landscapes and the predictability of evolution. Nat. Rev.

Genet. 15:480–490.

Visser JAGM, Hermisson J, Wagner GP, Meyers LA, Bagheri-Chaichian H, Blanchard JL, Chao L, Cheverud JM, Elena SF, Fontana W, et al. 2003. Perspective: Evolution and detection of genetic robustness. Evolution 57:1959–1972.

Wright S. 1932. The Roles of Mutation, Inbreeding, Crossbreeding and Selection in Evolution. 1:356–366.

Wu NC, Dai L, Olson CA, Lloyd-Smith JO, Sun R. 2016. Adaptation in protein fitness landscapes is facilitated by indirect paths. Elife 5:e16965.

Wu NC, Olson CA, Du Y, Le S, Tran K, Remenyi R, Gong D, Al-Mawsawi LQ, Qi H, Wu T-T, et al. 2015. Functional Constraint Profiling of a Viral Protein Reveals Discordance of Evolutionary Conservation and Functionality. PLOS Genet. 11:e1005310.

Wu NC, Young AP, Al-Mawsawi LQ, Olson CA, Feng J, Qi H, Chen S-H, Lu I-H, Lin C-Y, Chin RG, et al. 2014. High-throughput profiling of influenza A virus hemagglutinin gene at single-nucleotide resolution. Sci. Rep. 4:4942.

Wu NC, Young AP, Dandekar S, Wijersuriya H, Al-Mawsawi LQ, Wu T-T, Sun R. 2013. Systematic identification of H274Y compensatory mutations in influenza A virus neuraminidase by high-throughput screening. J. Virol. 87:1193–1199.

Wylie CS, Shakhnovich EI. 2011. A biophysical protein folding model accounts for most mutational fitness effects in viruses. Proc. Natl. Acad. Sci. 108:9916–9921.

Yampolsky LY, Stoltzfus A. 2005. The exchangeability of amino acids in proteins. Genetics 170:1459–1472.

Yang J-R, Chen X, Zhang J. 2014. Codon-by-Codon Modulation of Translational Speed and Accuracy Via mRNA Folding. PLoS Biol. 12:e1001910.

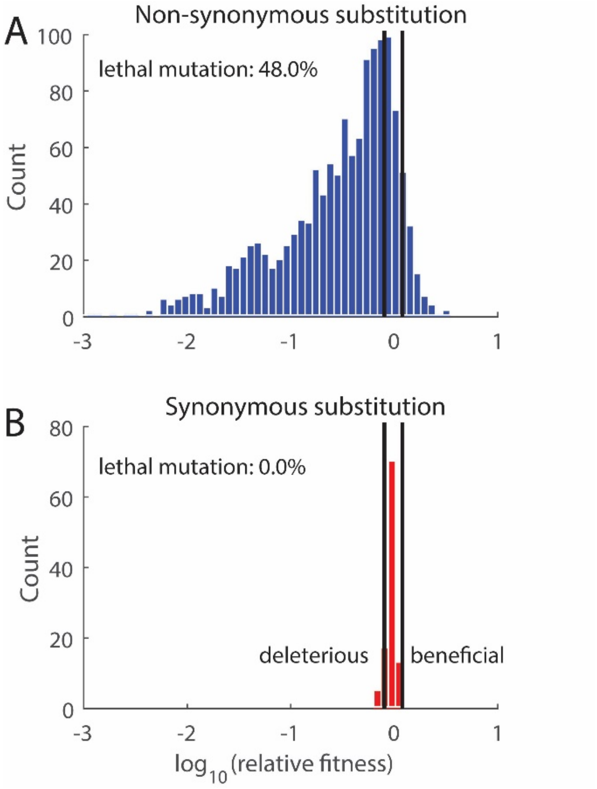

Figure 1. Distribution of fitness effects (DFE) of single codon substitutions of HCV NS5A protein. DFE of (A) non-synonymous substitutions and (B) synonymous substitutions. The thresholds (black lines) used for classifying beneficial, nearly neutral and deleterious mutations are determined by the variation of fitness values of synonymous substitutions (Methods). 88.7% of non-synonymous substitutions in NS5A protein are deleterious (among which 48.0% are lethal and not displayed in the histogram), 7.9% are nearly neutral and 3.4% are beneficial mutation.

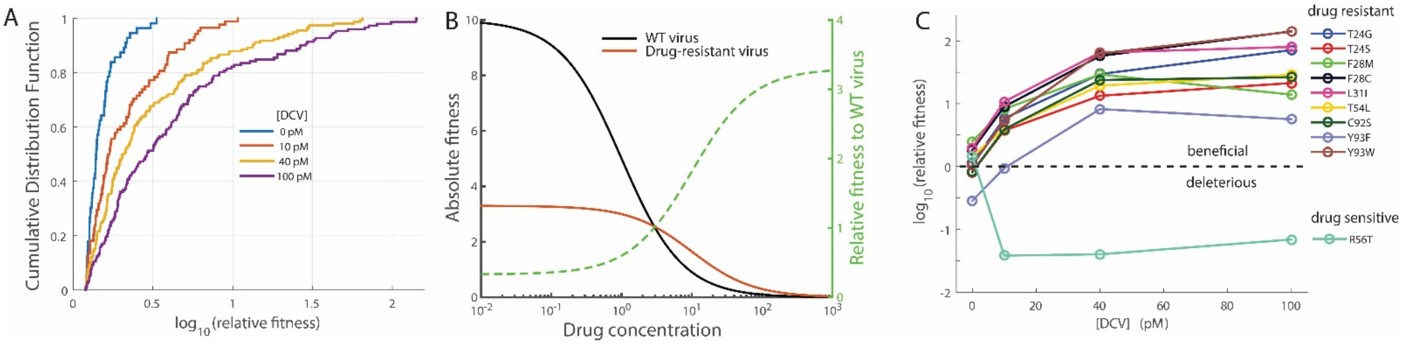

Figure 2. The spectrum of beneficial mutations shifts under the selection of an antiviral drug. (A) The cumulative distribution function of relative fitness of beneficial single amino acid substitutions under different selection conditions. (B) Hypothetical dose response curves of the wild-type virus and a drug-resistant mutant virus. Relative fitness of the drug-resistant mutant is expected to increase with drug concentration. (C) Relative fitness of validated drug resistant and sensitive mutations as a function of Daclatasvir concentration.

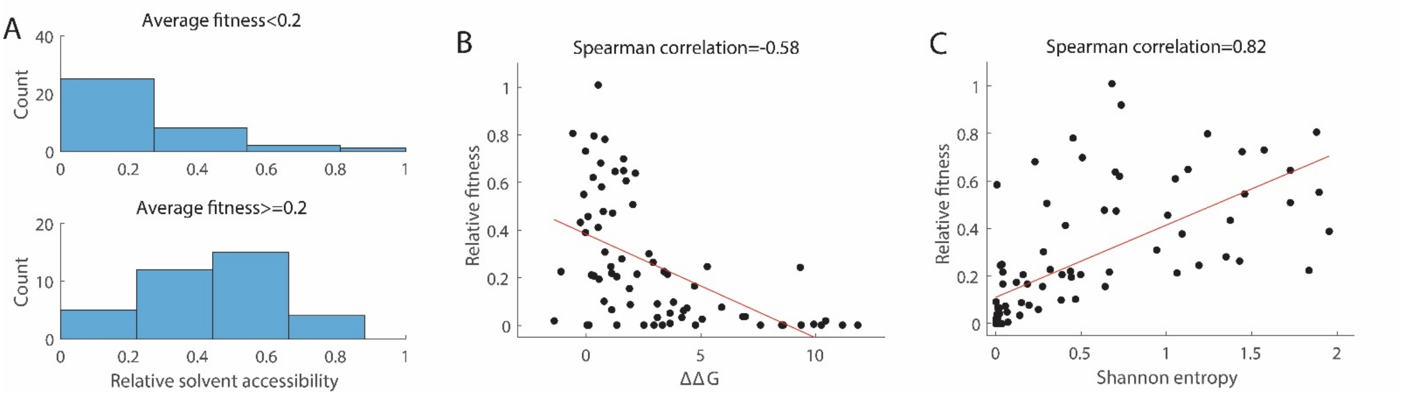

Figure 3. Deleterious mutations reveal constraints of protein evolution. (A) Amino acid sites that were less tolerant of mutations (average fitness of mutants <0.2) have lower relative solvent accessibility.. (B) Mutations that destabilized protein stability reduced the viral replicative fitness. Changes in folding free energy ΔΔG (Rosetta Energy Unit) of NS5A monomer were predicted by PyRosetta (Methods). The median of ΔΔG at each amino acid site is shown. (C) The within-patient sequence diversity of HCV NS5A protein at each site is highly correlated to the replicative fitness measured in cell line, suggesting that evolutionary pathways of viral proteins are indeed constrained by mutations that reduce viral replicative fitness. In (B) and (C), the average fitness of observed mutants at each amino acid site is shown. Red lines represent the fits by linear regression and are only used to guide the eye.

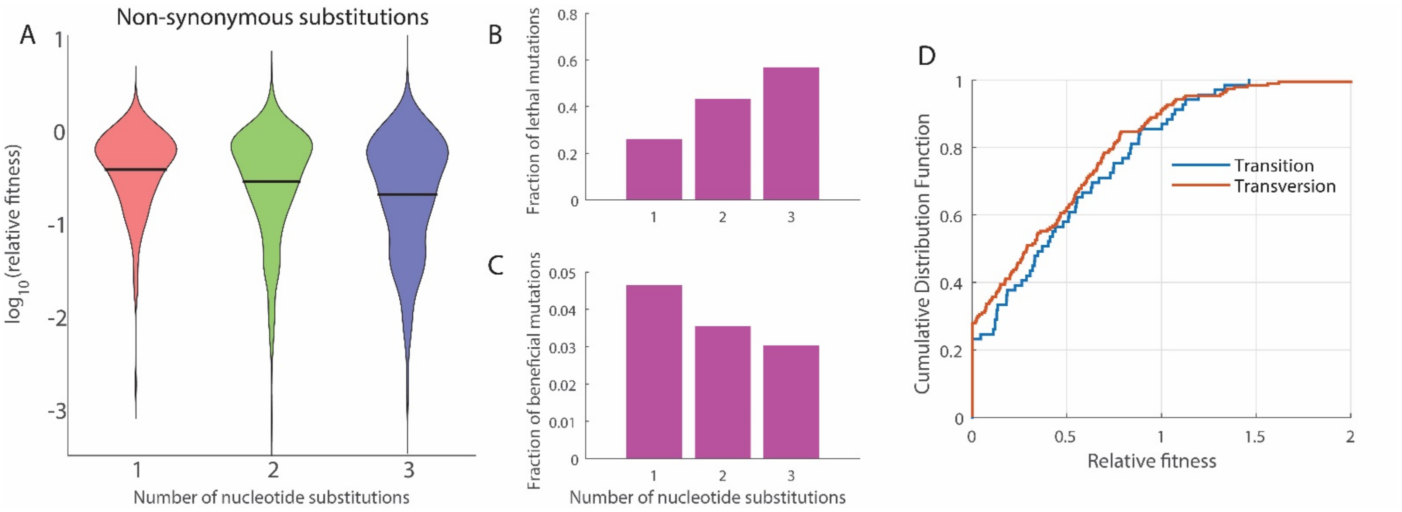

Figure 4. The role of the standard genetic code in viral evolution. (A) DFE of non-synonymous substitutions with 1, 2, and 3 nucleotide changes (lethal mutations are not displayed). Black lines indicates the mean. (B) The fraction of lethal mutations increases with the number of nucleotide changes, suggesting that the genetic code is optimized to buffer the mutational load (Chi-squared test, p=1.4×10^{-21}). (C) The fraction of beneficial mutations is slightly enriched for point mutations (Chi-squared test, p=0.41). Only non-synonymous substitutions are included in the analysis. (D) For non-synonymous point mutations, the fitness effect of transitions (n=69) is slightly less deleterious than that of transversions (n=190), but the difference is not significant (two-sample Kolmogorov-Smirnov test, p=0.53).

[DCV]	Fraction of beneficial codon substitutions	Scale parameter τ	Shape parameter κ	p-value
0 pM	3.4% (56/1634)	0.26	$0.27^{n.s.}$	0.09
10 pM	5.4% (88/1634)	0.63	0.62	0.0001
40 pM	9.7% (158/1634)	0.88	1.11	<0.0001
100 pM	9.3% (152/1634)	1.57	1.18	<0.0001

Table 1. Statistics of the distribution of fitness effects of beneficial single amino acid substitutions under varying selection pressure. n.s.: cannot reject the null hypothesis that the distribution is exponential (p>0.05).

Supplementary Materials

Supplementary Figures 1-11

Supplementary Tables 1-3

Supplementary Datasets 1

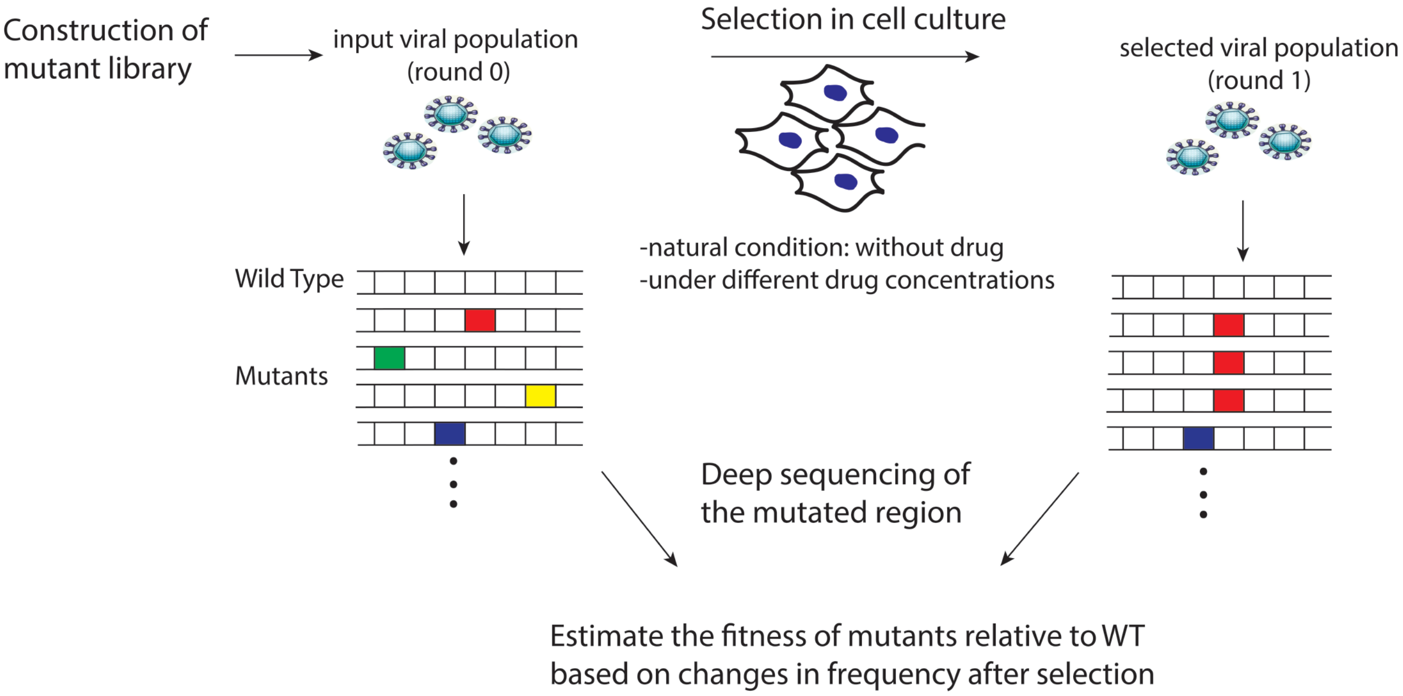
Construction of mutant library
input viral population (round 0)
Selection in cell culture
selected viral population (round 1)
Wild Type
Mutants
-natural condition: without drug
-under different drug concentrations
Deep sequencing of the mutated region
Estimate the fitness of mutants relative to WT based on changes in frequency after selection

Supplementary Figure 1. Experimental workflow of high-throughput fitness assays. We performed the selection of the mutant virus library using HCV cell culture system. Viral RNA was extracted after transfection or after selection, and reverse transcribed into cDNA. The mutated region in NS5A protein was amplified by PCR and sequenced by Illumina HiSeq. The relative fitness of a mutant virus to the wild-type virus was calculated based on the frequency of the mutant virus and the wild-type virus at round 0 (after transfection) and round 1 (after selection). See Methods for more details.

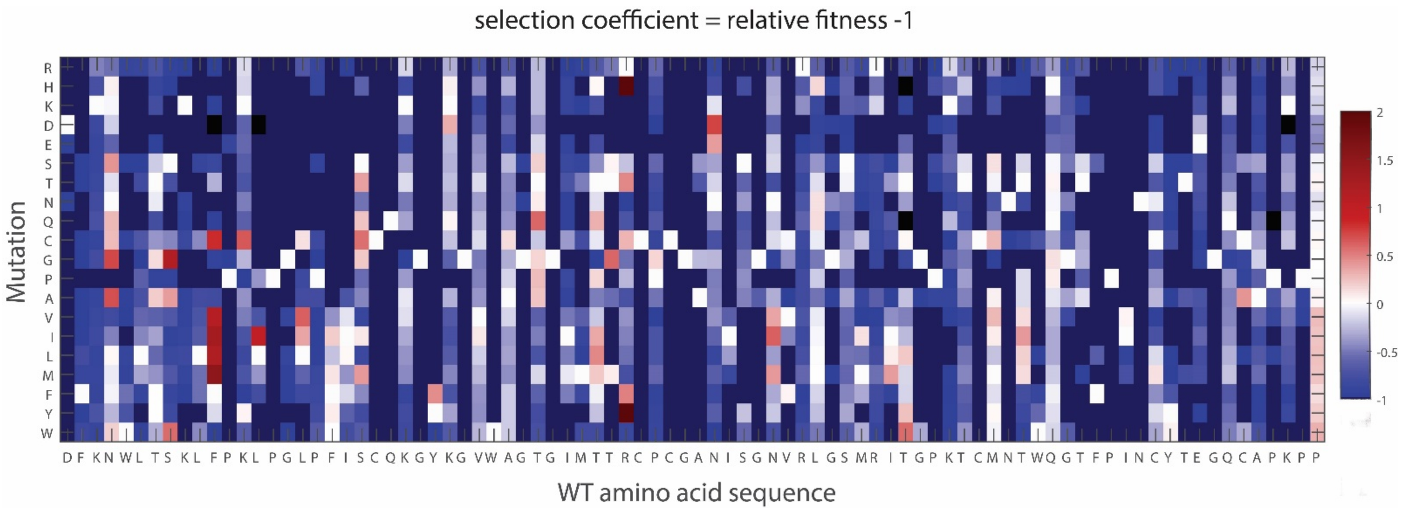

Supplementary Figure 2. Fitness effects of single amino acid substitutions in HCV NS5A protein under native condition. Different amino acid substitutions at the same site can have different fitness effects. The missing variants are colored black; lethal variants are colored dark blue.

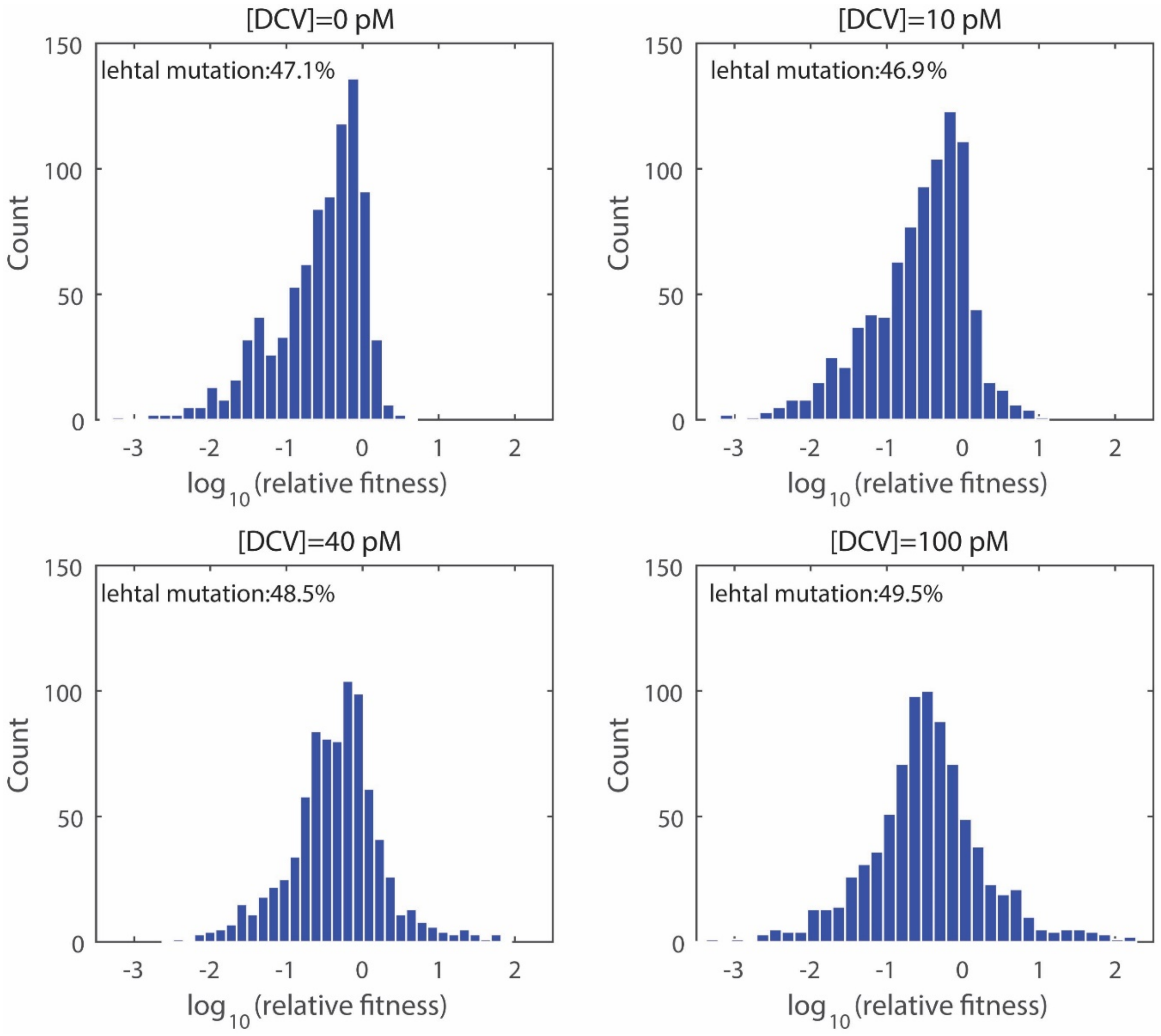

Supplementary Figure 3. DFE of non-synonymous substitutions under drug selection.

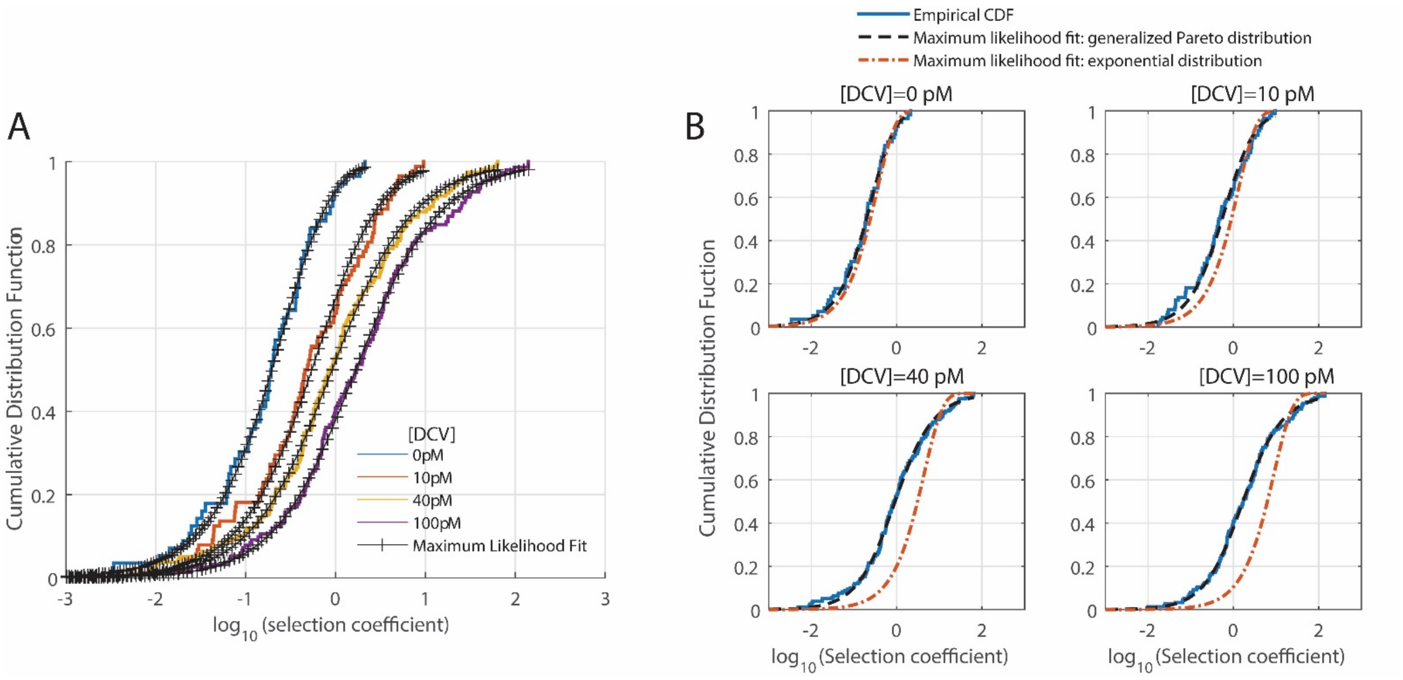

Supplementary Figure 4. Fitted distribution of fitness effects of beneficial single amino acid mutations. (A) Comparison of the fitted distribution to data. (B)The exponential distribution fails to fit the spectrum of beneficial mutations under conditions with drug selection.

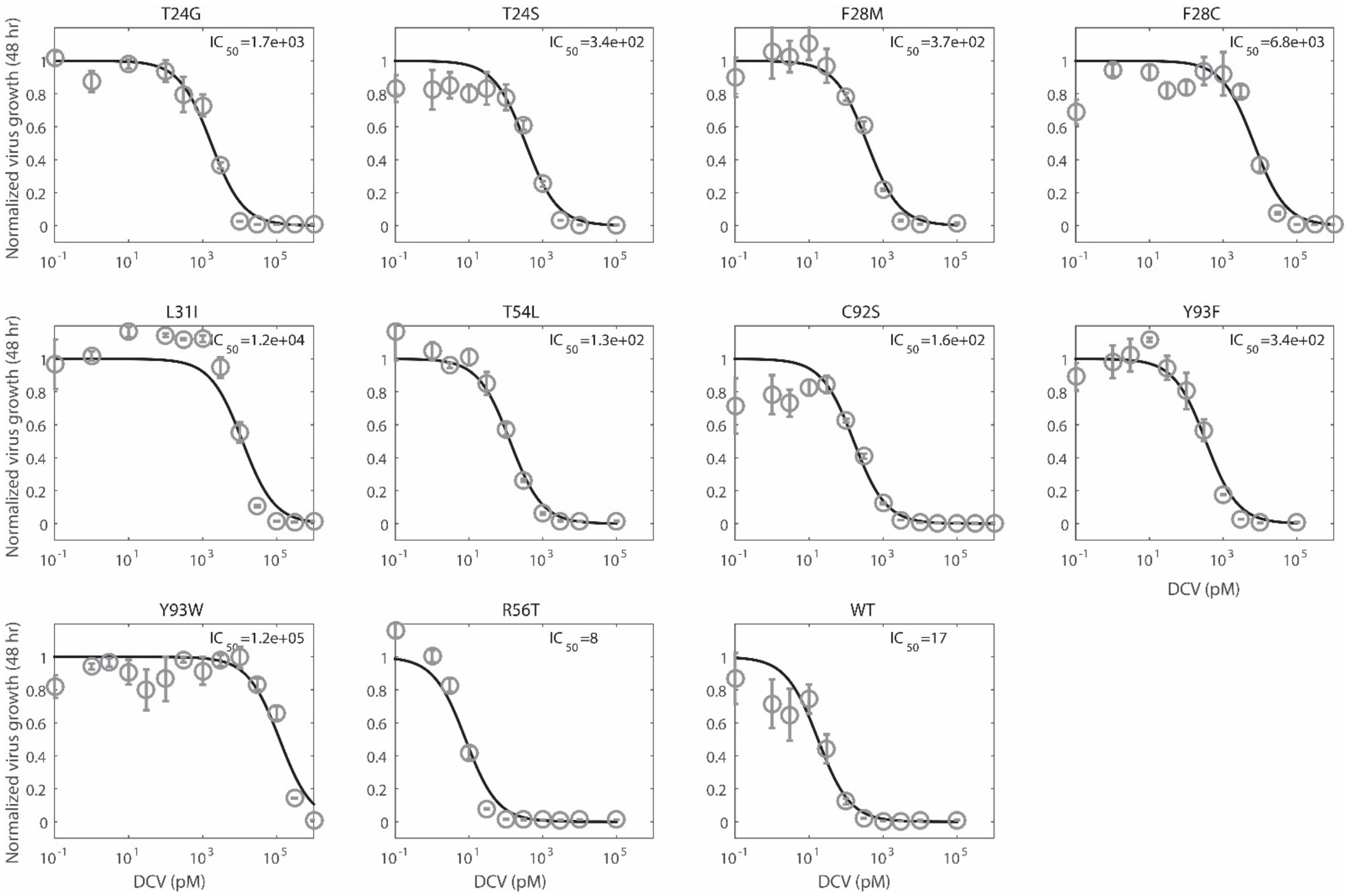

Supplementary Figure 5. Dose response curve of validated mutants (10 drug-resistant mutant, 1 drug-sensitive mutant) and WT virus. The Hill coefficient is fixed at 1 in fitting the dose response curves (Methods). The unit of IC_{50} is pM. The virus titer was measured after 48 hr of growth under drug treatment.

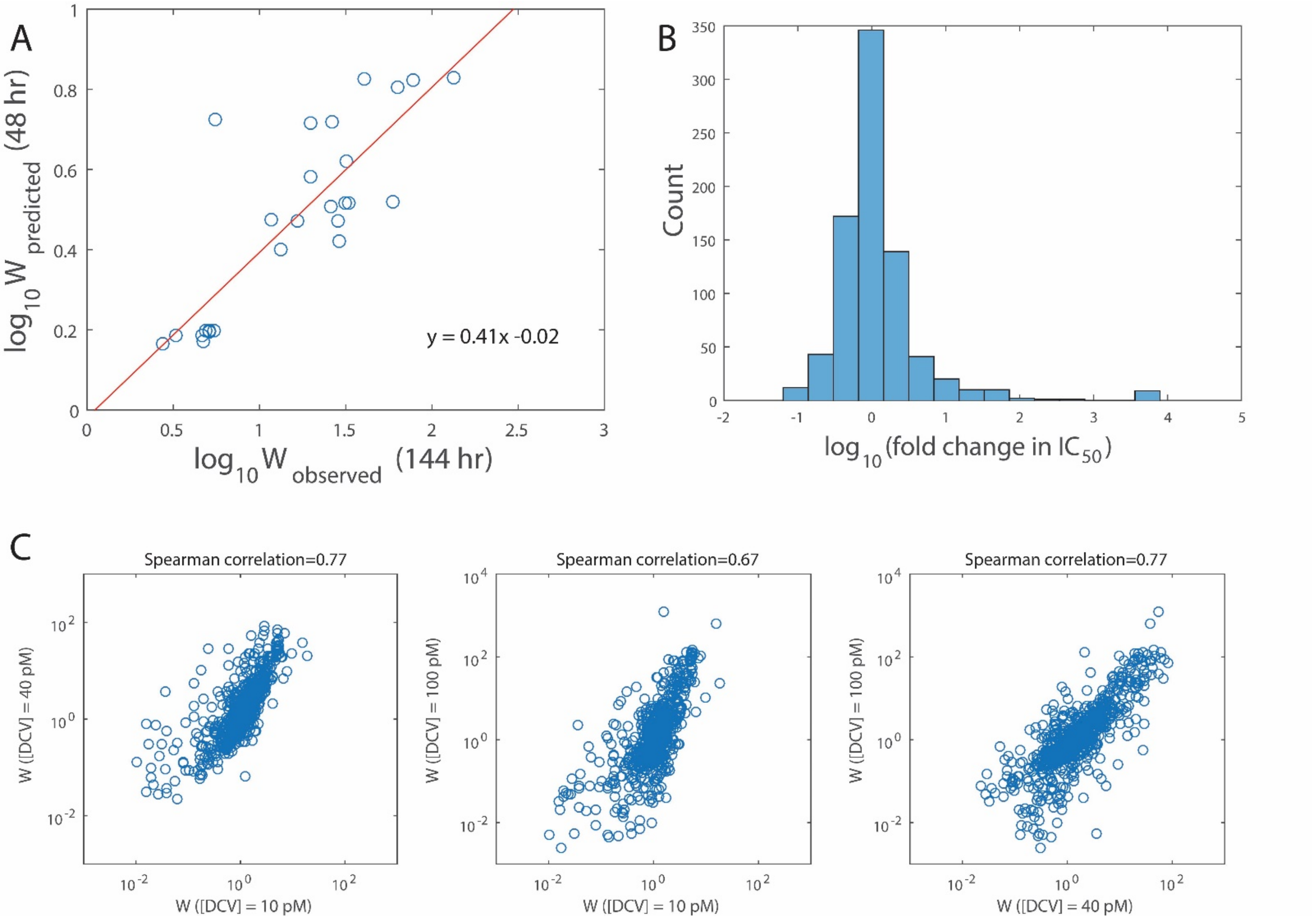

Supplementary Figure 6. Infer IC_{50} from fitness data under drug selection. (A) W is the fold change in relative fitness and represents the level of drug resistance relative to the wild type (Methods). Because the dose response curve depends on the duration of drug treatment, we normalized $W_{observed}$ (144 hr drug treatment in selection experiments) to $W_{predicted}$ (48 hr drug treatment, as used in the measurement of dose response curves of validated mutants). If viral growth is always exponential, the exponent is expected to be $\frac{48}{144} = \frac{1}{3}$. The fitted exponent is larger than $\frac{1}{3}$, suggesting that virus titer starts to saturate in 144 hr. (B) The fold change in IC_{50} caused by a single amino acid substitution is inferred from the measured fitness profiles under native condition and under drug selection (100 pM [DCV]). The existence of a group of highly resistant mutants (>10 fold change in IC_{50}) can explain why DFE of beneficial mutations shifts to a heavy-tailed distribution under drug selection. The resistance score of 9 single amino acid substitutions exceeds the maximum (Methods) and is manually set to 10^4 pM, which can be seen by the small peak in the right tail of histogram. (C) The measurement of drug resistance is consistent across different conditions of drug selection.

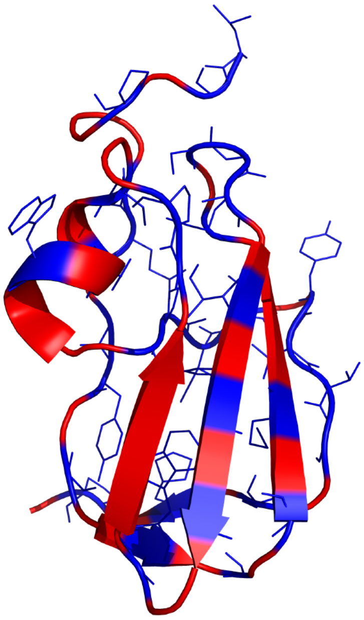

Supplementary Figure 7. Mutations at buried sites are highly deleterious. The structure of HCV NS5A monomer is visualized by PyMOL (PDB: 3FQM, chain A). Amino acid sites with an average fitness less than 0.2 are in blue and the corresponding side chains are shown.

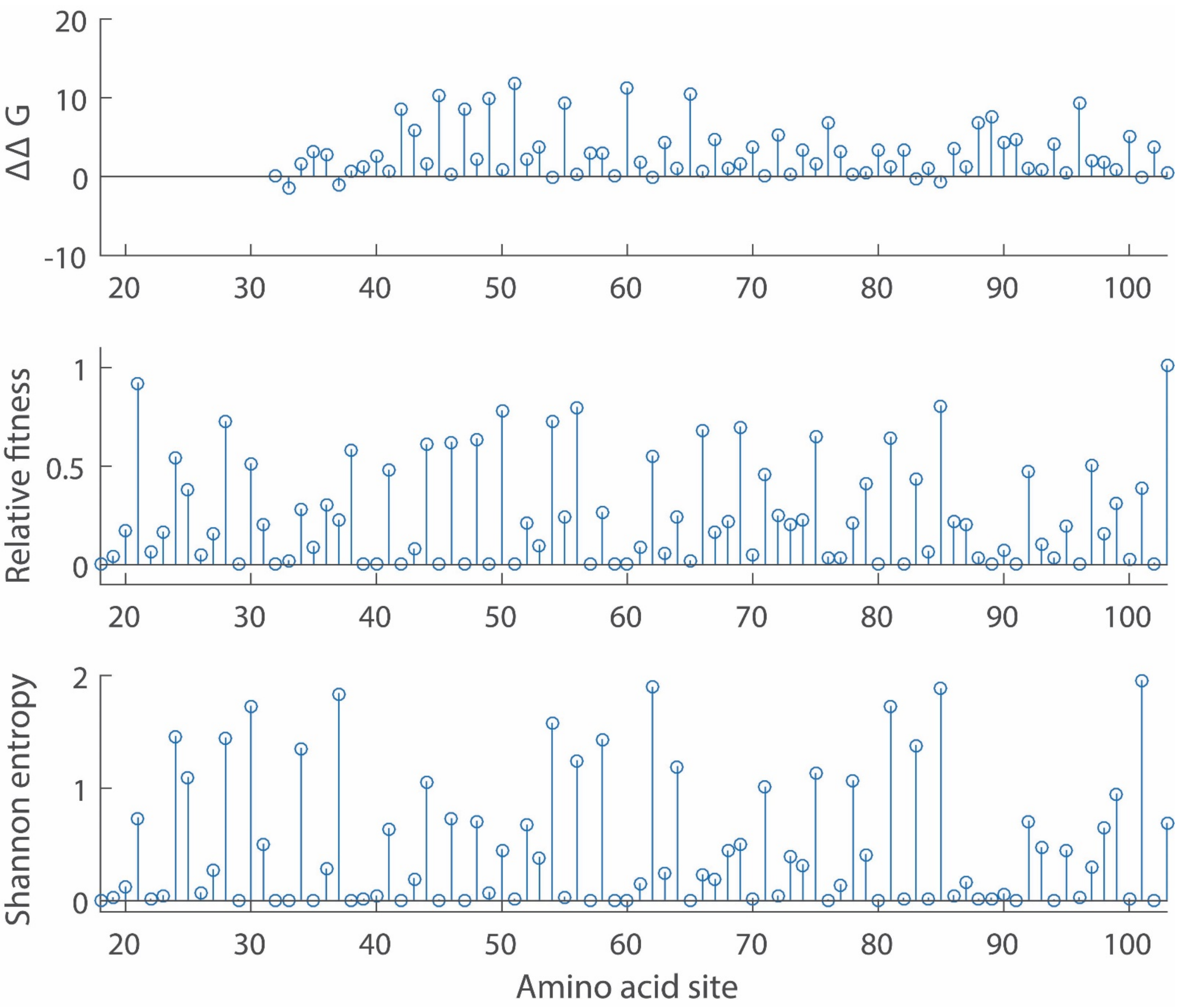

Supplementary Figure 8. Effects of mutations on protein stability, viral fitness and sequence diversity at each amino acid site. The fitness is averaged over all observed mutants at each amino acid site. The medium of ddG at each amino acid site is shown.

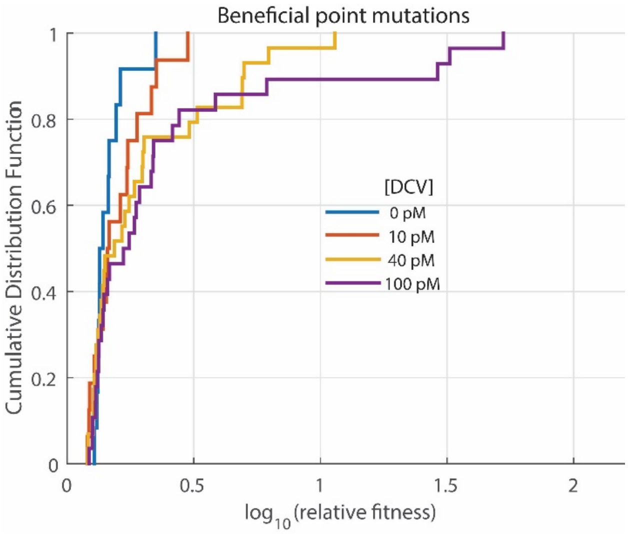

Supplementary Figure 9. Distribution of fitness effects of beneficial point mutations. Only non-synonymous mutations are included.

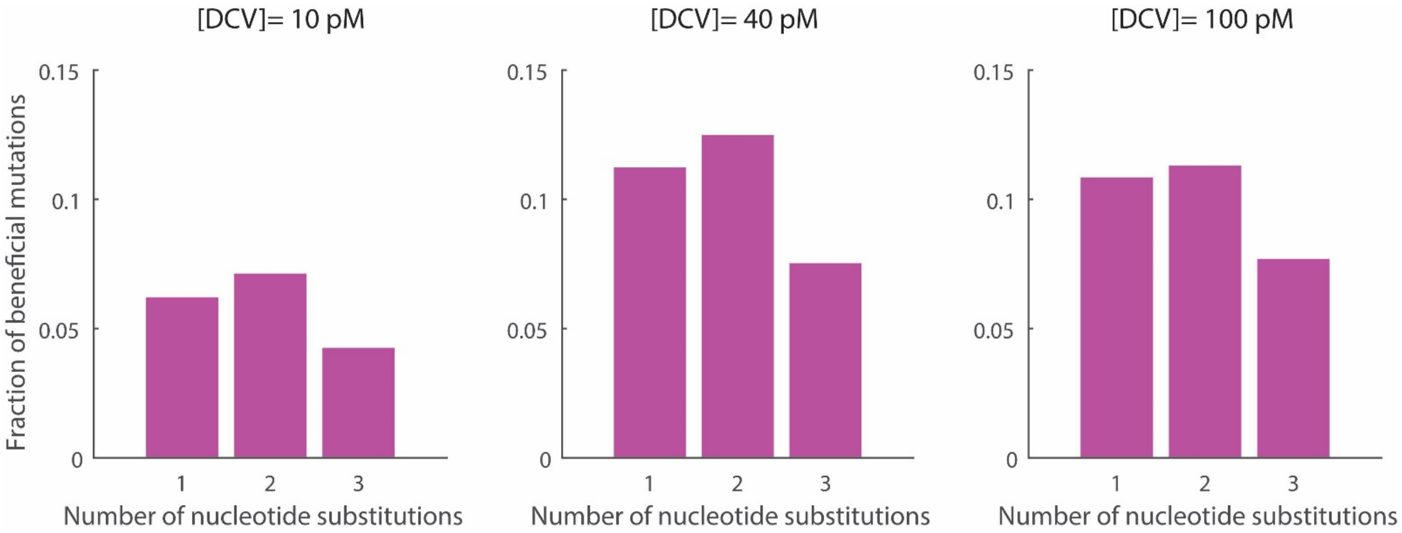

Supplementary Figure 10. The potential role of genetic code in adaptive mutations. For non-synonymous codon substitutions, the fraction of beneficial mutations with 3-nt changes is significantly lower than that of 1-nt or 2-nt mutations under drug selection (Pearson's chi-squared test: [DCV]=10 pM, $p=1.2\times10^{-2}$, 40 pM: $p=3.7\times10^{-4}$, 100 pM: $p=1.1\times10^{-2}$).

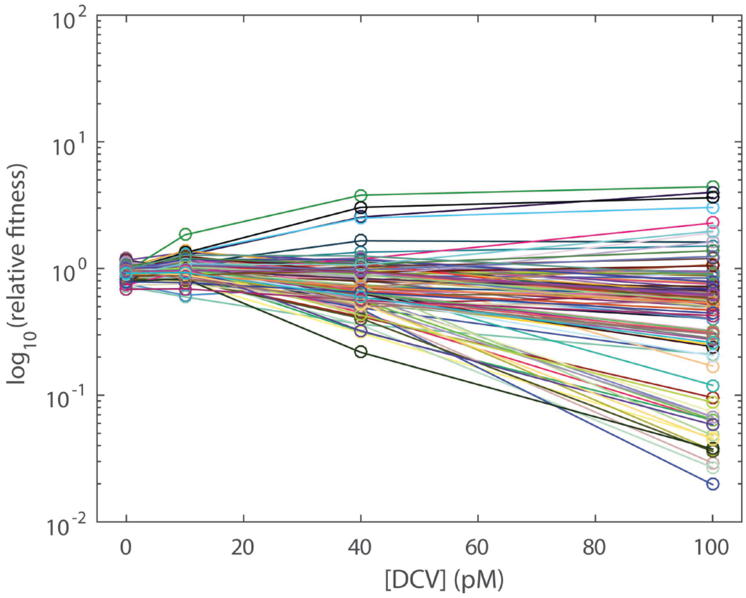

Supplementary Figure 11. Fitness effects of synonymous mutations under drug selection. Relative fitness of some synonymous mutations increased or decreased with drug concentration, suggesting that these mutations may have phenotypic effects on drug sensitivity.

[DCV]	Fraction of beneficial mutations	Scale parameter	Shape parameter	p-value
0 pM	4.6% (12/259)	0.13	$0.35^{\text{n.s.}}$	0.42
10 pM	6.2% (16/259)	0.41	$0.08^{\text{n.s.}}$	0.85
40 pM	11.2% (29/259)	0.32	1.06	0.0003
100 pM	10.8% (28/259)	0.32	1.50	<0.0001

Supplementary Table 1. Fitted parameters of the distribution of beneficial point mutations. Only non-synonymous mutations are included in the analysis. n.s.: p>0.05.

Library (amino acid site)	Forward primer	Reverse primer
1 (18-34)	5’-GTT TGC ACC ATC TTG ACA-3’	5’-TTG ACA AGA GAT GAA GGG-3’
2 (35-51)	5’-CAA GCT GCC CGG CCT C-3’	5’-GCA GCG CGT GGT CAT GAT-3’
3 (52-68)	5’-TGG GCC GGC ACT GGC-3’	5’-GAT CCT CAT AGA GCC CAG-3’
4 (69-85)	5’-CAT CTC TGG CA A TGT CCG C-3’	5’-AGC AAT TGA TAG GAA AGG CCC-3’
5 (86-103)	5’-TGC ATG AAC ACC TGG CAG-3’	5’-ATG GCG GTC TTG TAG TTC GT-3’

Supplementary Table 2. PCR primers used in preparation of sequencing samples.

Sample	**Barcode**
Plasmid	ATG
Transfection (round 0)	CCC
No drug (round 1)	CGG
[DCV]=10 pM (round 1)	CTT
[DCV]=40 pM (round 1)	ACT
[DCV]=100 pM (round 1)	AAC

Supplementary Table 3. Barcodes used in multiplexing Illumina sequencing samples.

Supplementary Dataset 1. Sequence of HCV NS5A protein.

Nucleotide sequence (amino acid site 18-103, “wild-type” in this study)

GACTTCAAAAATTGGCTGACCTCTAAATTGTTCCCCAAGCTGCCCGGCCTCCCCTTCATCTCTTGTCAAAAGGGGTACAAGGGTGTGTGGGCCGGCACTGGCATCATGACCACGCGCTGCCCTTGCGGCGCCAACATCTCTGGCAATGTCCGCCTGGGCTCTATGAGGATCACAGGGCCTAAAACCTGCATGAACACCTGGCAGGGGACCTTTCCTATCAATTGCTACACGGAGGGCCAGTGCGCGCCG

Amino acid sequence

DFKNWLTSKLFPKLPGLPFISCQKGYKGVWAGTGIMTTRCPCGANISGNVRLGSMRITGPKTCMNTWQGTFPINCYTEGQCAP